Title

High-Capacity, Cooperative CO2 Capture in a Diamine-Appended Metal—Organic Framework through a Combined Chemisorptive and Physisorptive Mechanism

Journal

Journal of the American Chemical Society, 146(9)

ISSN

0002-7863

Authors

Zhu, Ziting

Tsai, Hsinhan

Parker, Surya T

et al.

Publication Date

2024-03-06

DOI

10.1021/jacs.3c13381

Peer reviewed

Mechanochemically Accelerated Deconstruction of Chemically Recyclable Plastics

Mutian Hua[1], Zhengxing Peng[2], Rishabh D. Guha[3], Xiaoxu Ruan[3], Ka Chon Ng[4], Jeremy Demarteau[4], Shira Haber[1], Sophia N. Fricke[5], Jeffrey A. Reimer[5], Miquel Salmeron[1,4], Kristin A. Persson[1,3,4], Cheng Wang[2], Brett A. Helms[1,4,6]*

[1]Materials Sciences Division, Lawrence Berkeley National Laboratory, 1 Cyclotron Road, Berkeley CA, 94720 USA

[2]Advanced Light Source, Lawrence Berkeley National Laboratory, 1 Cyclotron Road, Berkeley CA, 94720 USA

[3]Department of Materials Sciences and Engineering, University of California Berkeley, Berkeley, CA 94720 USA

[4]The Molecular Foundry, Lawrence Berkeley National Laboratory, 1 Cyclotron Road, Berkeley CA, 94720 USA

[5]Department of Chemical and Biomolecular Engineering, University of California Berkeley, Berkeley, CA 94720 USA

[6]Chemical Sciences Division, Lawrence Berkeley National Laboratory, 1 Cyclotron Road, Berkeley CA, 94720 USA

*Correspondence: bahelms@lbl.gov

Abstract

Plastics redesign for circularity has primarily focused on how monomers should be configured to permit deconstruction at reasonable rates and ensure recovery in high yield and purity. Yet, during deconstruction, polymer chains interact with themselves and their reaction medium, introducing new context and urgency for understanding how the reactivity of polymers differs from that of small molecules. Here, we show that when polymers are deconstructed as solids in an acidolytic medium that swells the polymer, the rate of chain cleavage is accelerated by over 6-fold beyond that for bond cleavage in small molecule analogues. To understand this behavior, we advance and apply in-situ X-ray, NMR, and Raman spectroscopic characterization alongside computational modeling and simulation, where we reveal ion-specific mechanisms for rate acceleration occurring at different length scales. These mechanisms relate to not only mechanochemical activation of polymer chains, but also the degree to which acid anions modulate the structure and activity of water in stride with bond activation in solvent-separated ion pairs. Since residence time in reactors affects the economics of plastics recycling, understanding factors governing polymer deconstruction rates emerges as critically important, enabling the circular economy.

Main

Closed-loop chemical recycling of plastic waste to reusable monomers can be undertaken with low carbon and energy intensity when mechanically recycled plastics are deconstructed as solids, suspended in a liquid reaction medium[1–9]. During deconstruction, various species from the reaction medium partition into amorphous regions within the polymer, swelling the polymer and triggering chemical transformations therein. Yet, it remains a significant challenge to monitor and track reactions occurring in solvated polymer solids, leaving opaque the effects of polymer–solvent interactions on polymer reactivity.

Here, we show by using in-situ near-edge X-ray absorption fine structure (NEXAFS) and nuclear magnetic resonance (NMR) spectroscopic analysis that the rate of polymer deconstruction, thought to be dictated exclusively by monomer designs[10–12], is substantially higher when the polymer chains are stretched due to swelling in the reaction medium. Furthermore, by exploiting kosmotropic (stabilizing hydrogen bonding between water molecules) and chaotropic (disrupting hydrogen bonding between water molecules) counterions in the reaction medium to control the degree of swelling, we can modulate the extent of mechanochemical activation of cleavable bonds at the network level in circular plastics, increasing initial rates by six-fold. Concurrent with these effects, in-situ Raman spectroscopy studies and molecular dynamics simulations show that counterions further influence deconstruction rates at the molecular level by altering the structure of water near the sites of bond cleavage, which dictates the extent of bond activation toward hydrolysis. By understanding these combined effects across scales, we reveal compelling, non-obvious pathways for expediting polymer deconstruction: mechanochemical activation of hydrolysable bonds enables faster conversion of swollen polymer solids to dispersed particulates in reactive liquid

media, which should be explicitly tailored to maximize hydrolysis rates yielding reusable monomers in high yield through bond activation in smaller molecular fragments.

This understanding is a departure from conventional wisdom that might otherwise seek to explain polymer reactivity using theoretical insights or kinetic studies of small molecule models, which rarely consider the combined influence of heterogeneity, macromolecular architecture, chain conformation, solvation, and speciation[10,11,13–15]. Furthermore, observations that mechanochemical activation of bonds in swollen polymers is important during the early stages of polymer deconstruction provide new lines of intrigue for mechanochemistry and its potential role in informing plastics redesign for circularity[16–19]. We also find that the selection of reaction medium itself would benefit from the breadth of knowledge guiding the use of kosmotropic and chaotropic ions when seeking control over solvation[20,21], nucleation[22–24], crystallization[25–27], particularly in water-participating catalytic reactions[28,29]. Doing so ensures that oligomer intermediates in chemical recycling of plastics can be more efficiently deconstructed to monomers at high rates and in high yield. This knowledge, when combined with information regarding the structure and activity of water alongside solvation-induced mechanochemical activation of polymer bonds, provides an unexpectedly clear vantage point that captures the underlying phenomena responsible for polymer deconstruction across scales and opens the door to new design concepts exploiting these behaviors in future plastics to enhance and ensure their recyclability.

Modular Platform for Controlling Polymer Swelling in Acidolytic Media

Polydiketoenamines (PDK) are an emerging family of highly recyclable polymers that are poised to replace several classes of difficult-to-recycle polymers, such as epoxy and polyurethane resins.

Polydiketoenamines are synthesized from a diverse array of polytopic triketone and amine monomers via "click" polycondensation reactions[8]. Segmental chain flexibility inherent to many polyetheramines enables the creation of polydiketoenamine elastomers that swell in acidolytic media, returning reusable monomers with high yield and purity[30]. Lacking, however, has been a means to control the extent of PDK swelling in aqueous acid, which may depend on crosslinking density as well as the choice of acid.

To create PDK elastomers **1**–**3** with controlled crosslinking density, we combined a simple ditopic triketone[8] monomer (TK **1**) with either one of three tritopic amine-terminated polypropylene glycol crosslinkers (triamine **1–3**)[31], whose number-average molar masses were $M_n \sim 440$ g mol^{-1}, 3000 g mol^{-1}, and 5000 g mol^{-1}, respectively (**Fig. 1b & Supplementary Figs. 1–3**). PDK elastomers therefrom were flexible and exhibited a broad range of mechanical properties, including tensile strength up to 4.02 ± 0.68 MPa and tensile strain up to 1730 ± 350%, similar to commercial epoxy resins as well as highly stretchable elastomers (**Fig. 1b, Supplementary Figs. 4–5**). However, PDK elastomers **1**–**3** are distinctive from commercial materials in that they are thermally re-processible and chemically recyclable in a fully-closed loop (**Supplementary Figs. 6–7**)[9].

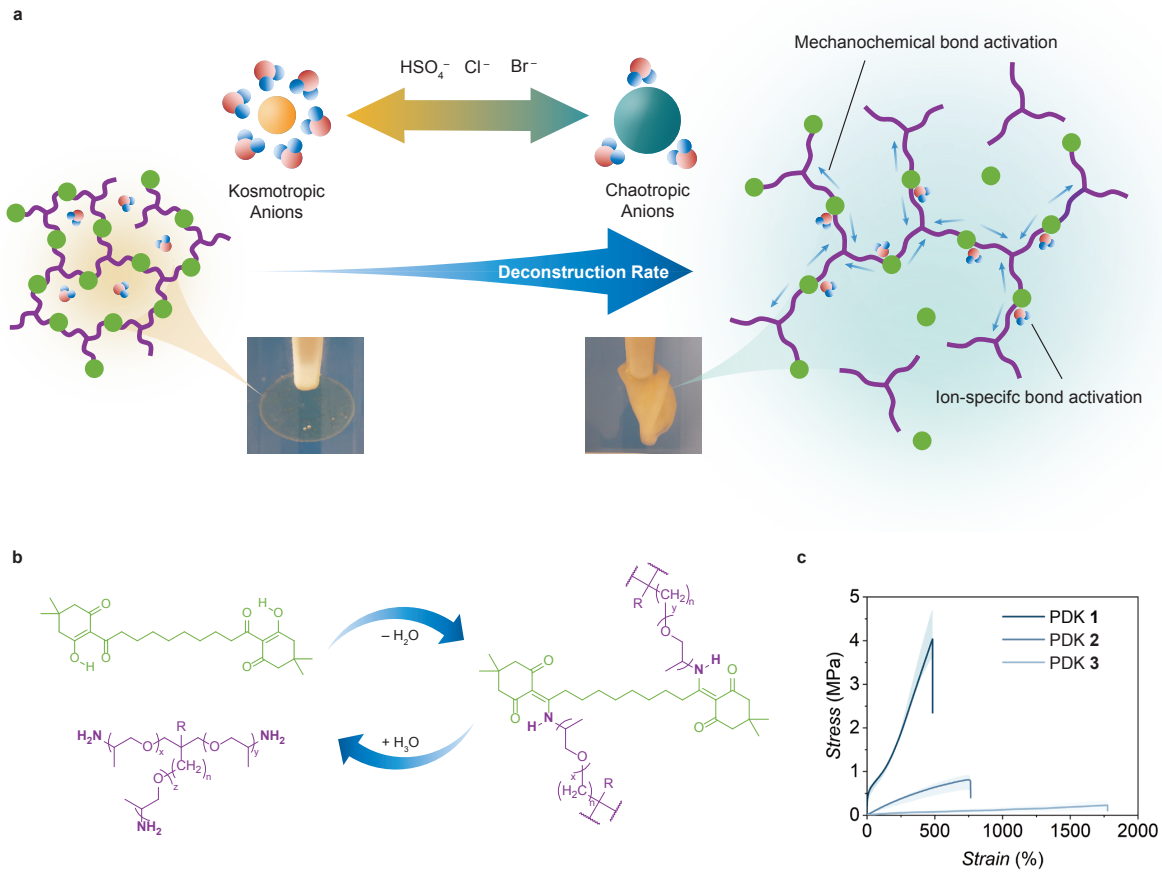

Fig.1 Enabling Circularity in Plastics by Accelerating Polymer Deconstruction Across Scales. a, At early stages of heterogeneous polymer deconstruction, controlling the swelling of polymer chains is key to accelerating reaction rates for bond hydrolysis. At longer time scales, the structure of water near the remaining hydrolysable bonds in the dispersed solids dictates rates through hydrogen bond-mediated bond activation. The acid counterion plays distinct roles during each phase of deconstruction: the chaotropicity of the anion can be exploited to control swelling, while its ability to engage in hydrogen bonding with water affects the solvation environment near the bond undergoing hydrolysis. The inset photos showed the appearance of PDK elastomer discs clamped by a tweezer undergoing deconstruction in 5.0 M H_2SO_4 (left) and 5.0 M HBr (right) for the same duration under ambient temperature. **b,** Chemical structure of circular PDK elastomers.

R is hydrogen, and *n* is one for triamine **1.** *R* is ethyl group, and *n* is zero for triamine **2** and **3**. **c,** Tensile stress–strain curves of PDK elastomers **1**–**3**. Error bars were calculated as the standard deviation from the mean for three independently tested samples for each PDK formulation.

Mechanochemical Acceleration of Polymer Network Deconstruction

To differentiate the reactivity of polymers (**Fig. 2a**) from small molecules (**Fig. 2b**) during deconstruction, we carried out in-situ NEXAFS in an X-ray transparent liquid cell to monitor initial rates of acidolysis in solid PDK elastomers in contact with prescribed amount of an aqueous acid. Aqueous acid ionizes diketoenamine functionality comprising the network, which in turn swells the polymer, in advance of hydrolysis reactions that ultimately generate triketone and triamine products. At ambient temperature, the hydrolysis reaction for this specific PDK network is slow, such that the X-ray set-up can be mounted without the PDK film experiencing significant chemical changes until triggered at the elevated temperature. The sensitivity of our methodology is dictated by the prevalence of spectroscopically distinctive chemical functionality in the reactants, intermediates, and products. Accordingly, we chose to study the effects of the reaction medium on deconstruction behaviors of elastomeric PDK **1**, owing to its higher concentration of diketoenamine bonds. To this end, we observed PDK **1** network deconstruction over 45 min at 60 °C, varying the acid as follows: 5.0 M H_2SO_4, 5.0 M HCl, and 5.0 M HBr (**Fig. 2c–e**). Prior to these experiments, we carried out extensive studies, modulating the incident X-ray flux to understand how best to minimize radiation damage to the sample as well as the volume of acid added to the in-situ cell to ensure signal-to-noise was adequate (**Supplementary Fig. 8**).

To interpret the data, we assigned features in the NEXAFS spectra by comparing them to simulated spectra for small molecule analogues of reactants, intermediates, and products by using time-dependent density function theory (TD-DFT)[32] (**Fig. 2f**, **Supplementary Fig. 9, 10**). We assigned the most prominent feature at 289.4 eV to C–N bonds exclusively present in liberated polyetheramine crosslinkers (i.e., acidolysis products), which enabled quantification of acidolysis rates. In contrast, less prominent features at 286.6 eV, corresponding to C=O bonds, were assignable to either diketoenamine moieties in PDK **1**–**3** (reactants) or liberated ß-triketones (products) and therefore less than ideal for precise quantification. To determine the initial rates of diketoenamine acidolysis, we thus calculated the peak areas at 289.4 eV and fit the data to a model for pseudo-first-order reaction kinetics (**Supplementary Fig. 11**). To our surprise, the initial rates for PDK deconstruction varied substantially by the composition of the acidolytic reaction medium: relative to the initial rate for PDK **1** deconstruction in 5.0 M H_2SO_4 ($-d$[DKE]/$dt = 4.22 \times 10^{-4}$ s^{-1}), those for its deconstruction in 5.0 M HCl and HBr were 62% and 90% faster, respectively (**Fig. 2g**).

To clarify the origin of rate acceleration, we assessed by variable temperature ^{1}H NMR the initial rates of diketoenamine acidolysis for an analogous small molecule diketoenamine, DKE **1**, dissolved in each of the different acids. We conducted these studies at temperatures of 40 °C, 60 °C, and 80 °C, extracting the initial rates and then fit the data to a pseudo-first-order kinetics model (**Fig. 2h**, **Supplementary Fig. 12–14**). In all cases, the initial rates of PDK **1** deconstruction (**Fig. 2g**) were substantially higher than the hydrolysis rates for DKE **1** in a given acidolytic medium at

a prescribed temperature (**Fig. 2h**), despite DKE **1** having more degrees of freedom as a dissolved solute than a diketoenamine bond would when part of a polymer network.

While the origin of this rate acceleration was not immediately clear, we observed differences in the degree of swelling depending on the acid type. Solvent up take in polymer networks leads to development of stress to balance the decrease in entropy[16,17], thus higher degree of swelling generates higher stress in the polymer network. Connecting the trend of swelling and rate of polymer deconstruction could imply a mechanochemical effect introduced by the kosmotropic or chaotropic characters of the different acid anions [20,33]. Consistent with this line of reasoning, the maximum swelling ratio increased in the order of HSO_4^-, Cl^-, and Br^- (**Fig. 2i**, **Supplementary Fig.15**). It is generally accepted that less-solvated chaotropic anions (Cl^-, Br^-) are driven to polymer–water interfaces, which in this case enhances swelling via more favorable solvation thermodynamics[21]. Most notably, we found a strong positive correlation between the ratio of initial rates of diketoenamine bond hydrolysis in networked PDK **1** to those of small molecule DKE **1** in different acidolytic media as a function of the swelling ratio. Thus, solvation of polymer networks leads to pronounced mechanochemical activation of hydrolysable bonds, regardless of the acid type; this effect is most pronounced in acidolytic media whose chaotropic anions collude with water to swell the network to the greatest extent (**Fig. 2j, k**). Likewise noteworthy is the apparent influence of acid type on acidolysis rates for small molecules featuring a diketoenamine bond (i.e., DKE **1**), which was unexpected (**Fig. 2h**).

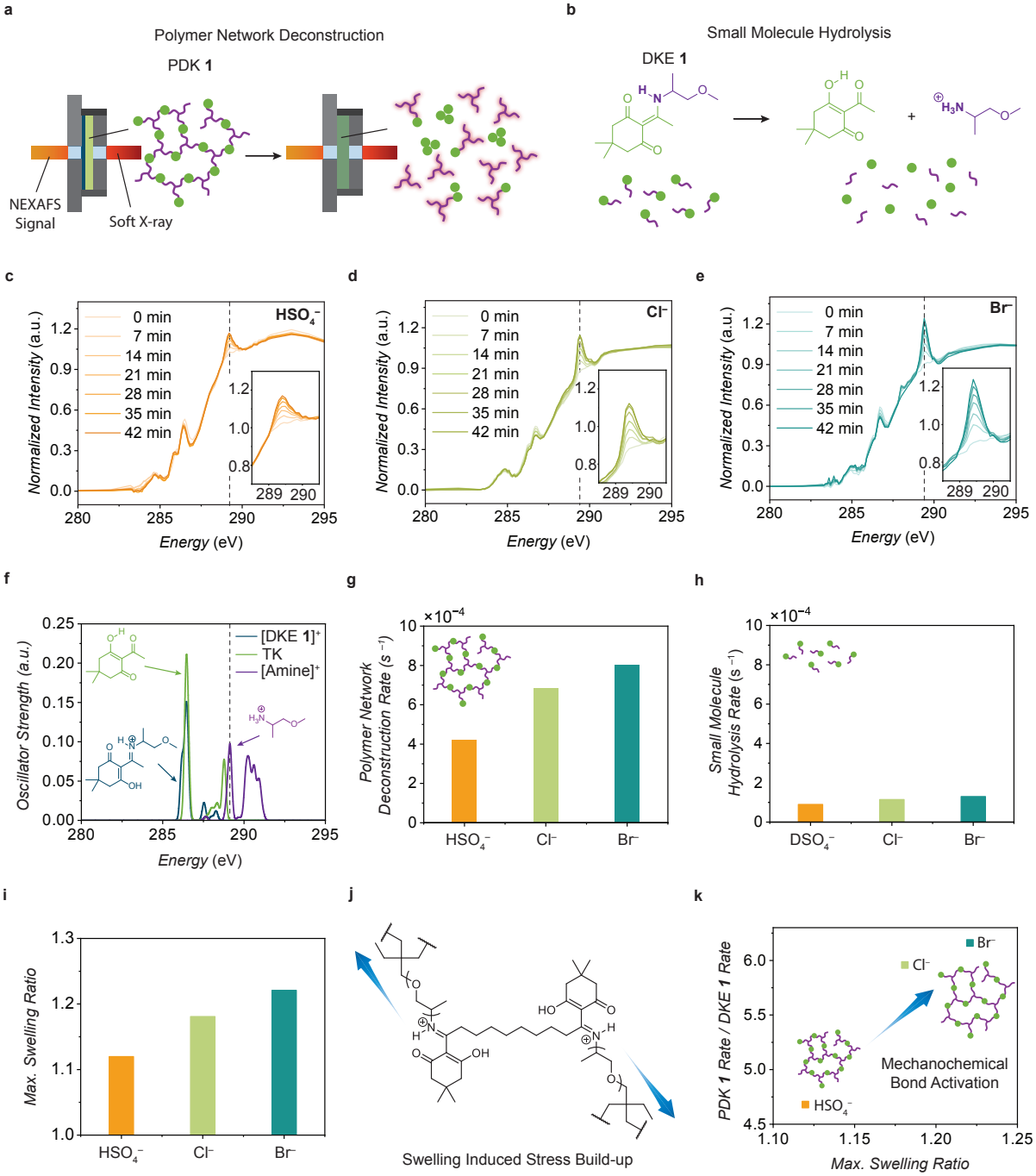

Fig. 2 Mechanochemical Activation of Hydrolysable Bonds in Solvated Polymer Networks. **a**, Illustration of the deconstruction of PDK elastomers during in-situ NEXAFS measurements. **b**, Illustration of the deconstruction of DKE **1**, a small molecule analogue of the hydrolysable bond in PDK elastomers. **c**–**e**, Overlaid NEXAFS spectra of PDK **1** undergoing deconstruction in 5.0 M

H_2SO_4, HCl and HBr. **f**, TD-DFT simulated NEXAFS spectrum of protonated DKE **1**, and 2-Acetyl-5,5-dimethyl-1,3-cyclohexanedione (TK), and 1-methoxy-2-propylamine, the acidolysis product of DKE **1**. **g**, Deconstruction rates of PDK **1** in 5.0 M H_2SO_4, HCl and HBr. **h**, Deconstruction rates of DKE **1** in 5.0 M D_2SO_4, DCl and DBr. **i**, Maximum swelling ratio of PDK **1** during deconstruction in 5.0 M H_2SO_4, HCl and HBr. **j**, Mechanochemical acceleration of diketoenamine acidolysis in solvated polymer networks. **k**, Ratio of deconstruction rates for PDK **1** and DKE **1** as a function of PDK elastomer swelling ratio in different acidolytic media.

Understanding Bond Activation in Solvent-Separated Ion Pairs

To understand the apparent role of acid type on molecular diketoenamine hydrolysis rates (**Fig. 2h**), we considered the effects of solvation and ion-pairing as well as the activity of water and their relation to bond activation in the rate-limiting step, where water adds to an iminium intermediate along the reaction coordinate. It was clear from the standard free energies of activation ($\Delta G^{\ddagger}$) for DKE **1** hydrolysis—which were extracted from temperature-dependent ^{1}H NMR kinetics experiments (**Fig. 3a**, **Supplementary Fig. 16**)—that the energy landscape for diketoenamine hydrolysis was substantially altered in different acidolytic media. We carried out MD simulations of DKE **1** in those media (i.e., with explicit solvent and acid molecules) and evidenced solvent-separated ion pairs, where a single water molecule was simultaneously bound to the iminium and any of the chaotropic halide ions through a series of hydrogen bonds (DKE **1** N–H···O, **Fig. 3b–d**). Furthermore, with increasing chaotropicity of the halide ions, we found that the number of hydrogen bonds between water molecules (Solvent H–O···H) was reduced (**Fig. 3b**), which is

concomitant with an increase in the activity of water towards participating in hydrolysis reactions, owing to the greater availability of oxygen lone pair electrons. Concurrently, the residence time of water molecules at the reaction center was increased (**Fig. 3c**). The confluence of increased bond activation in solvent-separated ion pairs, higher water activity, and longer residence time near bonds undergoing hydrolysis produced improved kinetics as well as thermodynamics for acidolysis with increasing chaotropicity of the acid anions.

Supporting these simulations, we found by Raman spectroscopy of DKE **1** in 5.0 M acid solutions (**Fig. 3e**) that the ionization of the diketoenamine bond is evident in the blue shift of the feature at 1375 cm^{-1} (characterized in water) to 1403–1410 cm^{-1} (characterized in acids), which was assigned to the C=N bond. With increasing chaotropicity of the acid anion (HSO_4^- < Cl^- < Br^- < I^-), the C=N bond was weakened characterized by an increasing red-shift in the peak position relative to the same peak observed in the least chaotropic acid (HSO_4^-) and therefore was more susceptible towards hydrolysis (**Fig. 3f**). This is consistent with stronger hydrogen bonds in solvent-separated ion pairs, *i.e.*, anion–water–NH(iminium)[34,35] . We also evidenced changes in the structure and activity of water in the region of 3100–3700 cm^{-1}. The O–H stretching band in all samples was composed of two principal components: the first at ~3200 cm^{-1}, corresponding to tetrahedral water with four hydrogen bonds (4 H-bond H_2O); the second at ~3440 cm^{-1}, corresponding to water with two hydrogen bonds (2 H-bond H_2O)[36,37]. With increasing chaotropicity of the anions, the tetrahedral structure of water was increasingly disrupted, as indicated by the diminution in the peak around 3200 cm^{-1}; the prevalence of higher-activity 2 H-bond H_2O features was increasingly dominant (**Fig. 3g**). This observation was further corroborated by Diffusion Ordered Spectroscopy (**Supplementary Table 1**) characterization of the same system, where increasing chaotropicity of

the acid anion led to increased diffusivity of hydroniums in the reaction medium, as a result of the increased activity of water. Thus, stronger H-bonds in solvent-separated ion pairs weakens the hydrolysable iminium bond, activating it towards acidolysis, while the structure of water is re-organized to show higher activity, promoting acidolysis (**Fig. 3h**).

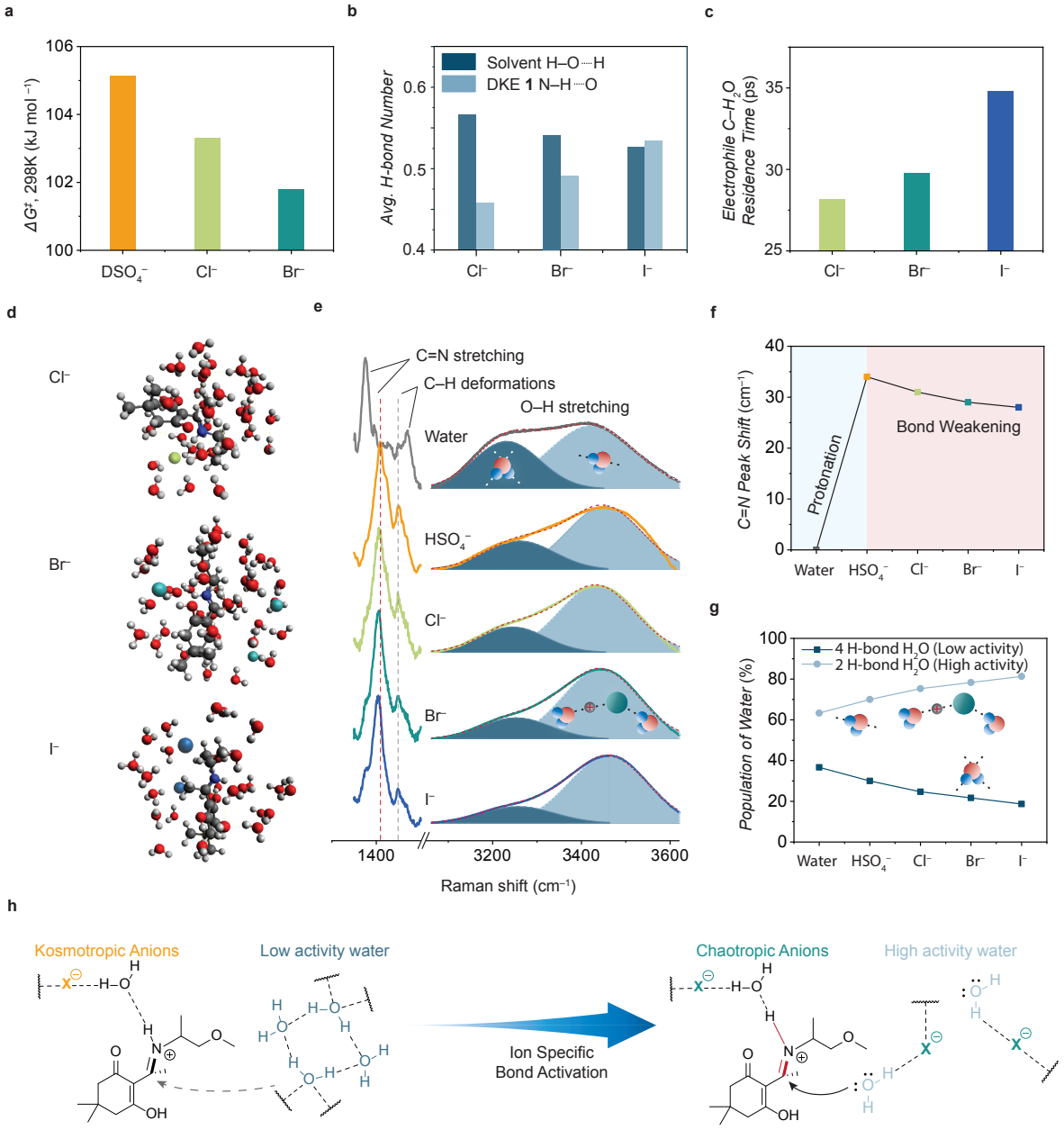

Fig. 3 Matched High Water Activity and Diketoenamine Bond Activation in Solvent-Separated Ion Pairs. a, Experimentally determined $\Delta G^{\ddagger}$ for DKE **1** hydrolysis in 5.0 M D_2SO_4,

DCl and DBr. **b,** Average number of hydrogen bonds (H-bond) per water molecule in bulk solvent, per DKE **1** near the iminium obtained from molecular dynamics (MD) simulations. **c,** Water residence time at the electrophile carbon of DKE **1** obtained from molecular dynamics (MD) simulations. **d,** Snapshots of the MD simulations for DKE **1** in different acidolytic media. **e**, Raman spectra of DKE **1** in deionized water and 5.0 M H_2SO_4, HCl, HBr, and HI. Gaussian distributions are shown in blue for species of water with different hydrogen bonding configurations. The red dotted line is the fitted spectrum, combining the two Gaussians. **f**, Shifts of C=N peak as a function of anion type. **g**, Population of 4 H-bond water and 2 H-bond water as a function of anion type. **h,** Illustration of bond activation due to the change in the structure of water. In the presence of chaotropic anions, stronger hydrogen bonds are formed between it, bound water, and the out-of-plane iminium species in solvent-separated ion pairs after the diketoenamine undergoes ionization in acid. Less hydrogen bonded water also exhibits higher activity during acidolysis.

Impacts of Accelerated Deconstruction Across Scales on Monomer Recovery

Understanding the implications of bond activation at the two length scales, we sought to control deconstruction of PDK elastomers by exploiting their interactions with the acidolytic reaction medium. At 60 °C, PDK **1** underwent deconstruction at different rates in 5.0 M HBr, HCl and H_2SO_4, which resulted in the progressive formation of smaller PDK solids (process 1) and ultimately colorless triketone precipitates (process 2) (**Fig. 4a**). While process 1 and 2 take place concurrently during PDK deconstruction, here we delineated the two processes for clarity of discussion. Processes 1 and 2 of PDK **1** deconstruction were fastest in 5.0 M HBr, where after only 1 h, triketone monomer had begun to precipitate from the reaction mixture; in 5.0 M HCl, this

onset took 2 h; in 5.0 M H_2SO_4, 3 h was required. While we observed similar trends with acid composition for PDK **2** (**Supplementary Fig. 17**) and PDK **3** (**Fig. 4b**), it was notable that process 1 was slower overall for networks with lower crosslinking density. Therefore, polymer networks with low crosslinking density (and concomitantly low volume fractions of ionizable functionality contributing to swelling) require tailored acidolytic media when it is desirable to accelerate their deconstruction via mechanochemical bond activation. For instance, the time to full disintegration of PDK **3** in 5.0 M H_2SO_4 and 5.0 M HCl was 7- and 3-times longer than that in 5.0 M HBr, respectively. Thus, the density of cleavable bonds within the network controls the rate at which bulk solids transform into smaller dispersed solids, allowing process 2 to proceed at rates dictated by surface area and the aforementioned polymer interactions with the acidolytic reaction medium vis-à-vis bond activation, water activity toward hydrolysis reactions, and water residence time near hydrolysable bonds.

In large reactors, where such transformations will eventually take place, stirring rates and residence times impact energy requirements for executing circularity at scale. The physical mechanisms described here are a means to tailor these to minimize such costs in the future, provided there are no discernable differences in the quality of recyclates produced by comparison to first-generation monomers. To verify this, we analyzed the purities and quantified the yields of TK **1** and triamine crosslinkers **1**–**3** recovered from deconstructed elastomeric PDK **1**–**3**, respectively, in each of the three acidolytic reaction media (**Supplementary Fig. 18**). In all cases, recovered TK **1** and triamine **1**–**3** were essentially indistinguishable from pristine monomers by ^{1}H NMR (**Fig. 4c**, **d**, **Supplementary Fig. 19–27**). The recovery yields were >90% with no obvious distinction between different acids. Thus, the interactions with polymers and acidolytic reaction media during polymer

deconstruction can be tailored to more quickly generate higher surface area particulates that are easier to distribute within a reactor with stirring, such that subsequent monomer generation in the final stages of hydrolysis benefits from increased surface area. More specifically, the first process of network deconstruction can be accelerated by mechanochemical effects tied to degree of swelling, while the second process can be accelerated by bond activation in solvent-separated ion pairs.

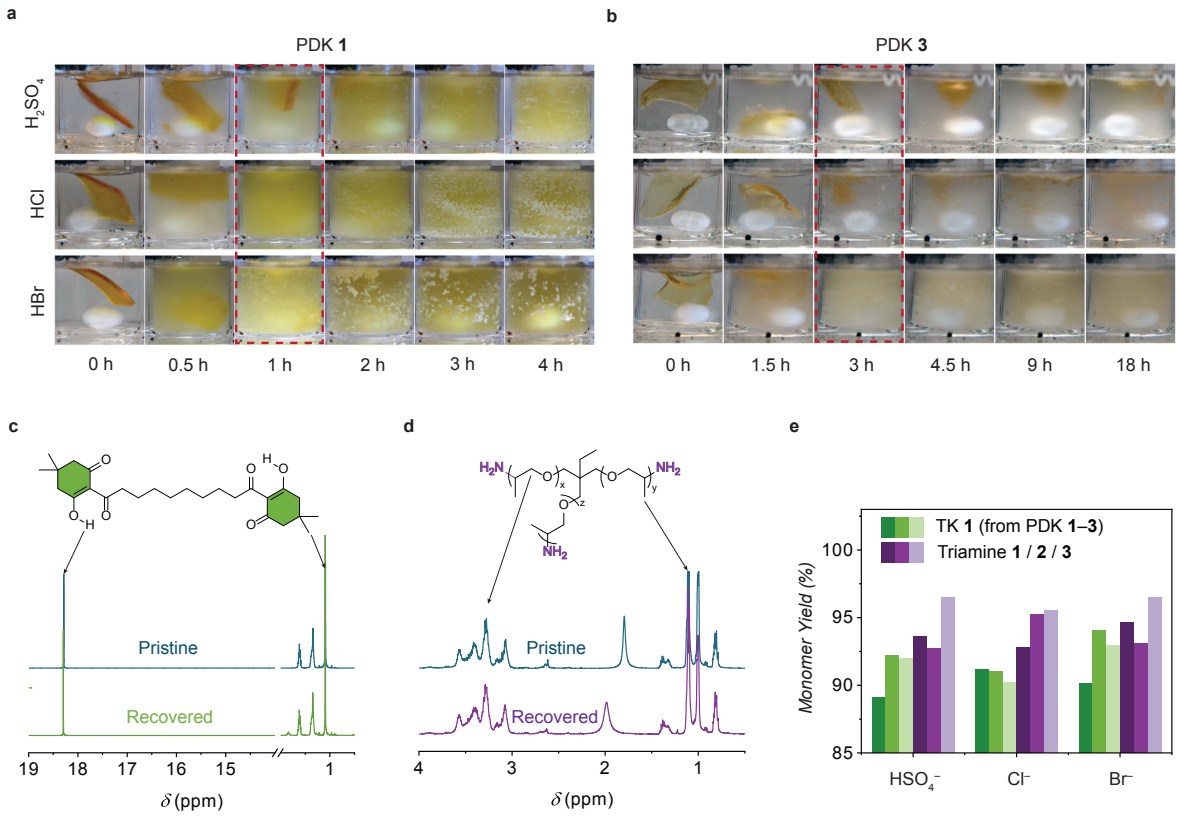

Fig. 4 Ion-Specific effects in PDK deconstruction in acid. a, Snap-shots of PDK **1** undergoing acidolytic deconstruction in 5.0 M H_2SO_4, HCl, and HBr. **b,** Snap-shots of PDK **3** undergoing acidolytic deconstruction in 5.0 M H_2SO_4, HCl, and HBr. **c,** ^{1}H NMR spectrum of pristine (top) and recovered (bottom) TK **1** from PDK **1** deconstructed in 5.0 M HCl. **d,** ^{1}H NMR spectrum of pristine (top) and recovered (bottom) triamine **1** from PDK **1** deconstructed in 5.0 M HCl. **e,** Yields

of recovered TK **1** and triamines **1**–**3** from PDK **1**–**3**, respectively, deconstructed in 5.0 M H_2SO_4, HCl and HBr.

Discussion

Deconstruction of polymer networks in acidolytic media reveals distinctive roles at different time and length scales played by network architecture and acid counterions. At early stages of deconstruction of macroscopic polymer solids, solvation and swelling of the network lead to an acceleration of deconstruction rates due to mechanochemical activation of hydrolysable bonds. Network swelling is enhanced for acid anions with increasing chaotropicity, resulting in initial rates that are up to 6-fold higher than those for small molecule analogues. As deconstruction proceeds, the influence of the reaction medium remains prominent due to the activation of hydrolysable bonds at the molecular scale, particularly in solvent-separated ion pairs; the activity of water also changes substantially with acid composition at high concentration, affecting rates in a manner which is matched to those of bond activation with different acid anions. These molecular-scale phenomena not only alter energy landscapes for bond hydrolysis ($\Delta\Delta G^{\ddagger}$ up to 3 kJ mol^{-1}), but also affect the water residence time near activated bonds and therefore the statistics of reactions producing reusable monomers. Thus, polymer–solvent interactions must be explicitly taken into account alongside monomer design when considering the fundamental and practical basis for recycling efficiency and circularity in plastics. Moreover, these interactions can now be accounted for by implementing workflows that combine synthetic chemistry, advanced in-situ characterization, and computational simulations at their relevant length and time scales.

Supporting Information

Supporting Information is available from the publisher website or from the author.

Acknowledgements

This work was funded by the U.S. Department of Energy, Office of Science, Office of Basic Energy Sciences, Materials Sciences and Engineering Division under contract no. DE-AC02-05-CH11231, Unlocking Chemical Circularity in Recycling by Controlling Polymer Reactivity across Scales program CUP-LBL-Helms. Work at the Molecular Foundry—including polymer synthesis, characterization, X-ray liquid cell assembly, Raman spectroscopy characterization—was supported by the Office of Science, Office of Basic Energy Sciences, of the U.S. Department of Energy under Contract No. DE-AC02-05CH11231. Work at the Advanced Light Source—including NEXAFS—was supported by the Office of Science, Office of Basic Energy Sciences, of the U.S. Department of Energy under the same contract. This research used the Savio computational cluster resource provided by the Berkeley Research Computing program at the University of California, Berkeley (supported by the UC Berkeley chancellor, vice chancellor for research, and chief information officer). We thank Norman Su and Huntsman Corp. for providing the triamine monomers used in the study.

Author Contribution

B.A.H contributed to the conceptualization of the project. B.A.H and M.H. contributed to the design of the project. B.A.H and J.D. contributed to the design of the PDK elastomer. M.H., Z.P and C.W. contributed to the design, experiment, and data analysis of NEXAFS characterization. R.D.G. contributed to the TD-DFT simulations of NEXAFS spectra. X.R. contributed to the MD simulations. M.H and K.C.N contributed to the experiment and data analysis of Raman spectroscopy. M.H., S.H., and S.N.F. contributed to the NMR characterization and analysis. B.A.H. and M.H. contributed to visualization. B.A.H. and M.H. wrote the original draft. All authors contributed to the final draft and editing. B.A.H, C.W., K.A.P., M.S., J.A.R. supervised research, provided project administration, and acquired funding.

Conflict of Interest

B.A.H. is an inventor on the U.S. provisional patent application 62/587,148 and submitted by Lawrence Berkeley National Laboratory that covers PDKs, as well as aspects of their use and recovery. E.A.D., J.D.K., A.R.E., K.A.P., and B.A.H. are inventors on the U.S. provisional patent application 63/390,962 submitted by Lawrence Berkeley National Laboratory that covers elastomeric PDKs, as well as aspects of their use and recovery. B.A.H. has a financial interest in Cyklos Materials and Sepion Technologies. The authors declare that they have no other competing interests.

Data Availability Statement

The data that support the findings of this study are available from the corresponding author upon reasonable request.

References

1. Coates, G. W. & Getzler, Y. D. Y. L. Chemical recycling to monomer for an ideal, circular polymer economy. *Nat Rev Mater* **5**, 501–516 (2020).
2. Abel, B. A., Snyder, R. L. & Coates, G. W. Chemically recyclable thermoplastics from reversible-deactivation polymerization of cyclic acetals. *Science* **373**, 783–789 (2021).
3. Häußler, M., Eck, M., Rothauer, D. & Mecking, S. Closed-loop recycling of polyethylene-like materials. *Nature* **590**, 423–427 (2021).
4. Sathe, D. *et al.* Olefin metathesis-based chemically recyclable polymers enabled by fused-ring monomers. *Nat Chem* **13**, 743–750 (2021).
5. Zhou, L. *et al.* Chemically circular, mechanically tough, and melt-processable polyhydroxyalkanoates. *Science* **380**, 64–69 (2023).
6. Wang, X. *et al.* Healable, Recyclable, and Mechanically Tough Polyurethane Elastomers with Exceptional Damage Tolerance. *Advanced Materials* **32**, 2005759 (2020).
7. Manker, L. P. *et al.* Sustainable polyesters via direct functionalization of lignocellulosic sugars. *Nat Chem* **14**, 976–984 (2022).
8. Christensen, P. R., Scheuermann, A. M., Loeffler, K. E. & Helms, B. A. Closed-loop recycling of plastics enabled by dynamic covalent diketoenamine bonds. *Nat Chem* **11**, 442–448 (2019).
9. Helms, B. A. Polydiketoenamines for a Circular Plastics Economy. *Acc Chem Res* **55**, 2753–2765 (2022).

10. Epstein, A. R., Demarteau, J., Helms, B. A. & Persson, K. A. Variable Amine Spacing Determines Depolymerization Rate in Polydiketoenamines. *J Am Chem Soc* **145**, 8089 (2023).
11. Demarteau, J. *et al.* Circularity in mixed-plastic chemical recycling enabled by variable rates of polydiketoenamine hydrolysis. *Sci Adv* **8**, 8823 (2022).
12. Demarteau, J. *et al.* Biorenewable and circular polydiketoenamine plastics. *Nat Sustain* **6**, 1426–1435 (2023).
13. Young, J. B. *et al.* Bulk depolymerization of poly(methyl methacrylate) via chain-end initiation for catalyst-free reversion to monomer. *Chem* **9**, 2669–2682 (2023).
14. Ellis, L. D. *et al.* Chemical and biological catalysis for plastics recycling and upcycling. *Nat Catal* **4**, 539–556 (2021).
15. Chu, M., Liu, Y., Lou, X., Zhang, Q. & Chen, J. Rational Design of Chemical Catalysis for Plastic Recycling. *ACS Catal* **12**, 4659–4679 (2022).
16. Metze, F. K., Sant, S., Meng, Z., Klok, H. A. & Kaur, K. Swelling-Activated, Soft Mechanochemistry in Polymer Materials. *Langmuir* **39**, 3546–3557 (2023).
17. Lee, C. K. *et al.* Solvent swelling activation of a mechanophore in a polymer network. *Macromolecules* **47**, 2690–2694 (2014).
18. Beedle, A. E. M. *et al.* Forcing the reversibility of a mechanochemical reaction. *Nat Commun* **9**, 3155 (2018).
19. Wang, J. *et al.* Mechanical Acceleration of Ester Bond Hydrolysis in Polymers. *Macromolecules* **55**, 10145–10152 (2022).
20. Zhang, Y., Furyk, S., Bergbreiter, D. E. & Cremer, P. S. Specific ion effects on the water solubility of macromolecules: PNIPAM and the Hofmeister series. *J Am Chem Soc* **127**, 14505–14510 (2005).
21. Bruce, E. E. & Van Der Vegt, N. F. A. Molecular Scale Solvation in Complex Solutions. *J Am Chem Soc* **141**, 12948–12956 (2019).
22. He, Z. *et al.* Tuning ice nucleation with counterions on polyelectrolyte brush surfaces. *Sci Adv* **2**, (2016).
23. Guo, Q. *et al.* Tuning Ice Nucleation and Propagation with Counterions on Multilayer Hydrogels. *Langmuir* **34**, 11986–11991 (2018).
24. He, Z. *et al.* Bioinspired Multifunctional Anti-icing Hydrogel. *Matter* **2**, 723–734 (2020).
25. Zhang, H., Wang, W., Mallapragada, S., Travesset, A. & Vaknin, D. Ion-Specific Interfacial Crystallization of Polymer-Grafted Nanoparticles. *Journal of Physical Chemistry C* **121**, 15424–15429 (2017).
26. Wu, S. *et al.* Ion-specific ice recrystallization provides a facile approach for the fabrication of porous materials. *Nat Commun* **8**, 15154 (2017).
27. Hua, M. *et al.* Strong tough hydrogels via the synergy of freeze-casting and salting out. *Nature* **590**, 594–599 (2021).
28. Resasco, J. *et al.* Promoter Effects of Alkali Metal Cations on the Electrochemical Reduction of Carbon Dioxide. *J Am Chem Soc* **139**, 11277–11287 (2017).
29. Zhang, H., Gao, J., Raciti, D. & Hall, A. S. Promoting Cu-catalysed CO2 electroreduction to multicarbon products by tuning the activity of H_2O. *Nat Catal* **6**, 807–817 (2023).
30. Dailing, E. A. *et al.* Circular Polydiketoenamine Elastomers with Exceptional Creep Resistance via Multivalent Cross-Linker Design. *ACS Cent Sci* (2023) doi:10.1021/acscentsci.3c01096.

31. Polyetheramines: Huntsman Corporation (HUN). https://www.huntsman.com/products/detail/354/polyetheramines.
32. Timoshenko, J. & Roldan Cuenya, B. In Situ/ Operando Electrocatalyst Characterization by X-ray Absorption Spectroscopy. *Chem Rev* **121**, 882–961 (2021).
33. Chen, X., Yang, T., Kataoka, S. & Cremer, P. S. Specific ion effects on interfacial water structure near macromolecules. *J Am Chem Soc* **129**, 12272–12279 (2007).
34. Ghosh, N., Roy, S., Bandyopadhyay, A. & Mondal, J. A. Vibrational Raman Spectroscopy of the Hydration Shell of Ions. *Liquids* **3**, 19–39 (2022).
35. Fulton, J. L. & Balasubramanian, M. Structure of hydronium (H3o+)/chloride (Cl -) contact ion pairs in aqueous hydrochloric acid solution: A zundel-like local configuration. *J Am Chem Soc* **132**, 12597–12604 (2010).
36. Sun, Q. The Raman OH stretching bands of liquid water. *Vib Spectrosc* **51**, 213–217 (2009).
37. Wang, Y.-H. *et al.* In situ Raman spectroscopy reveals the structure and dissociation of interfacial water. *Nature* **600**, 81–85 (2021).